Chapter 36

Polybenzoxazine/Carbon Nanotube Composites

M.G. Mohamed, R.-C. Lin and S.-W. Kuo[1]
National Sun Yat-Sen University, Kaohsiung, Taiwan
[1]Corresponding author: e-mail: kuosw@faculty.nsysu.edu.tw

Chapter Outline

1 INTRODUCTION

It is well known that a carbon atom has six protons in its nucleus and six electrons in its outer shell and that its electronic configuration occupies the $1s^2$, $2s^2$, and $2p^2$ atomic orbital. There are many types of carbon bonded materials, such as graphene, fullerenes, and carbon nanotubes (CNTs) [1–4], which have attracted industrial and academic interests because of their unique mechanical and thermophysical properties. CNTs are defined as hollow cylinders consisting of a single or multiple sheets of graphene wrapped into a cylinder stabilized and held together through π-stacking force. There are two popular kinds of CNTs: single-walled carbon nanotubes (SWCNTs) and multi-walled-carbon nanotubes (MWCNTs) [5]. SWCNTs consist of a single sheet of graphene rolled seamlessly to a form a cylinder with a diameter of 1 nm. MWCNTs consist of an array of cylinders formed and separated by 0.35 nm with diameters from 2 to 100 nm. The advantages of sp^2 carbon atoms include the ability to build layers with strong van der Waals interactions between those layers [6–9]. Many methods have been developed for the preparation and fabrication of CNTs, including chemical vapor deposition (CVD) [10,11], the laser ablation [12], and the carbon arc discharge techniques [13,14].

CNTs were discovered in 1991 by Iijima. Nowadays, it is difficult to find a material that exhibits balanced properties in all mechanical, thermal, and electrical areas such as CNTs. Pristine CNTs possess densities around 100 MA/cm^2 and also high carrier mobilities of 105 cm^2/Vs, which ascribe to their homogeneous structure and their charge carriers that can easily move through nanotubes [15–18]. In addition, CNTs show mechanical properties analogous to graphite (such as elastic modulus and stiffness) because graphite structure and CNTs possess a Young's modulus at approximately 1.06 TPa. Furthermore, Young's modulus is strongly independent of diameter and CNT type. On the other hand, MWCNTs possess a Young's modulus of 200–4000 GPa, an axial flexural strength of 14 GPa, and an axial compression strength of 100 GPa [19–25]. Although CNTs have attracted much attention in many areas because of their high potential for application, the insolubility and difficulty in the dispersion of CNTs in organic solvents have thus far limited real-life uses of CNTs. Two approaches can enhance the dispersion of CNTs in many organic solvents

Advanced and Emerging Polybenzoxazine Science and Technology. http://dx.doi.org/10.1016/B978-0-12-804170-3.00036-6

and can improve the properties of CNTs. They include functionalization through (1) covalent bonding [26–29] and (2) physical bonding [30–33] at the CNT surface.

As just mentioned, there are two approaches to enhance the homogeneous dispersion of CNTs into a polymer matrix. The first approach, the modification and functionalization of CNTs through a covalent bond, allows a functional group to be connected at the ends of the sidewalls of the CNTs to enhance their dispersion and solubility in organic solvents and polymeric matrices. The chemical modification of CNT surfaces has been performed by an oxidation process (HNO_3). This oxidative treatment leads to open tubes with the functionalized sidewall and tube ending with a carboxyl group (COOH). The covalent functionalization of the CNT will alter the hybridization of carbon atoms from sp^2 to sp^3, thereby disrupting or destroying their electrical conductivity. The strategies for the covalent grafting of polymer chains to CNTs can be divided into "grafting from" and "grafting to" methods [34,35]. The grafting from method places the covalently bonded initiators on the CNT's tube surface, followed by polymerization of monomers to form polymer chains that are bound to the tubes. The advantage of this method is that it gives the surface-grafted CNT a high grafting density. The grafting to approach is based on the already polymerized chain that has reactive chain ends that attach the CNT surface. The disadvantage of the grafting to method is that the primary linking of the polymer chains sterically hinders the diffusion of additional molecules to the surface, which leads to low grafting density. The second physical interaction approach typically involves van der Waals and π-π interactions between organic molecules/polymers and CNT without any influence on the electronic network of the CNT.

Benzoxazine resins, a new class of phenolic resins, were developed recently and attracted academic and industrial interest because of their low cost, ease of processing, and high performance. All monomer-containing oxazine rings undergo ring-opening polymerization simply through heating without an added initiator and/or catalyst. Polybenzoxazines also possess many unique properties: low water uptake, low surface-free energies, and high glass-transition temperatures. The improvements in the properties of polybenzoxazines were required; so it is necessary to prepare polybenzoxazines-CNTs nanocomposites and to combine the attractive properties of polybenzoxazines and CNTs [36–39]. In this chapter, we focus on the preparation of polybenzoxazine/(MWCNT or SWCNT) nanocomposites through covalent functionalization and noncovalent interaction through π-π stacking interactions.

2 CHARACTERIZATION OF MODIFIED MWCNT AND SWCNT THROUGH COVALENT INTERACTION

From the purification studies of CNT, we know that the yield of CNT depends strongly on the oxidation or reduction time, the oxidation or reduction agent, and temperature. Yu et al. modified the MWCNT through a covalent approach with nitric acid, after which the acid-treated MWCNT was filtered and washed several times with deionized water. Finally, the crude product was added to a mixture of toluene diisocyanate (TDI) and $Sn(Oct)_2$ as a catalyst, as shown in Scheme 1 [40]. In addition, Yu et al. provided many examples of modified polybenzoxazines/CNT nanocomposites using the covalent interaction approach [41].

2.1 Characterization of the Modified MWCNT by HNO_3 and After Modified With TDI

The MWCNT modified by HNO_3 and TDI was characterized by Fourier transform infrared spectroscopy (FTIR). The main characteristic absorption bands appeared at 3400, 2700, 1705, and 1173 cm^{-1}, which corresponded with the OH, COOH, C═O, and C—O groups, respectively. In addition, the band at 3300 cm^{-1} was assigned to the secondary amine from the amide group; the band at 2272 cm^{-1} was due to the isocyanate group, —N═C═O; and the band at 1705 cm^{-1} appeared because of the C═O stretching mode of carboxyl group, indicating that the successful modification of the CNT's surface took place. To confirm the proposed chemical structure of the modified MWCNT surface, as shown in Scheme 1, the modified CNT was also investigated by ^{1}H-NMR analysis. The ^{1}H NMR spectra of the HNO_3-treated MWCNT and the TDI-treated MWCNT show the signals at 2.02 and 7.70 ppm for OH and COOH protons, respectively. In addition, the characteristic signals of the aromatic protons, CONH and CH_3, were detected at 7.02–7.17, 6.38, and 2.23 ppm, respectively.

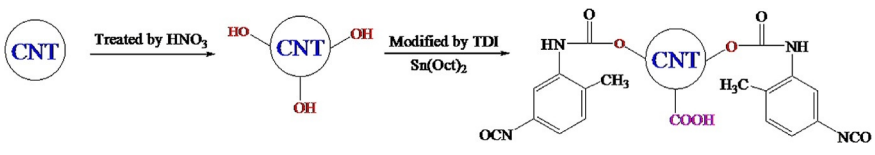

SCHEME 1 The modified MWCNT with HNO_3 and TDI. *Reprinted with permission from Q. Chen, R.W. Xu, D. Yu. Multiwalled carbon nanotube/polybenzoxazine nanocomposites: preparation, characterization and properties, Polymer 47 (2006) 7711–7719.*

3 PREPARATION OF POLYBENZOXAZINE-CNT NANOCOMPOSITES THROUGH COVALENT INTERACTION

In this section, we focus on the preparation of polybenzoxazine/CNT composites through a covalent bond formation at the polymer matrix/CNT interface. For example, Yu et al. first proposed the modification of a MWCNT surface by a HNO_3 and TDI treatment and prepared the poly(BA-a)/MWCNT nanocomposites via a solvent method [40]. They found highly homogeneous dispersion and adhesion of MWCNTs in a polybenzoxazine matrix, possibly because of a reaction between the isocyanate groups and the hydroxyl group after ring-opening of benzoxazine, as shown in Scheme 2. After polymerization at an elevated temperature, the 2275, 1231, and 945 cm^{-1} bands that corresponded to the N═C═O stretching, asymmetric C—O—C, and tri-substituted benzene ring stretching disappeared, and two new bands formed at 1619 and 1480 cm^{-1} were due to the NHCO group from the reaction between N═C═O and phenolic OH of polybenzoxazine and the tetrasubstituted benzene ring appeared as a result of covalent bond formation at the interface and polymerization of the benzoxazine resin.

4 PROPERTIES OF POLYBENZOXAZINE-CNT NANOCOMPOSITES THROUGH COVALENT INTERACTION

4.1 Properties of Poly(BA-a)-CNT Nanocomposites

Fig. 1 shows the dispersion of MWCNT within the BA-a matrix was investigated by scanning electron microscopy (SEM). The fracture surface and uniform dispersion of 1 or 2 wt% of MWCNT in the polybenzoxazine matrix with a small area of the extended white structures are shown in Fig. 1A and B. Fig. 1C and D shows the SEM images of various concentrations of MWCNT inside the polybenzoxazine matrix, where homogeneous dispersion of MWCNT on a nanoscale is observed. Fig. 1C and D

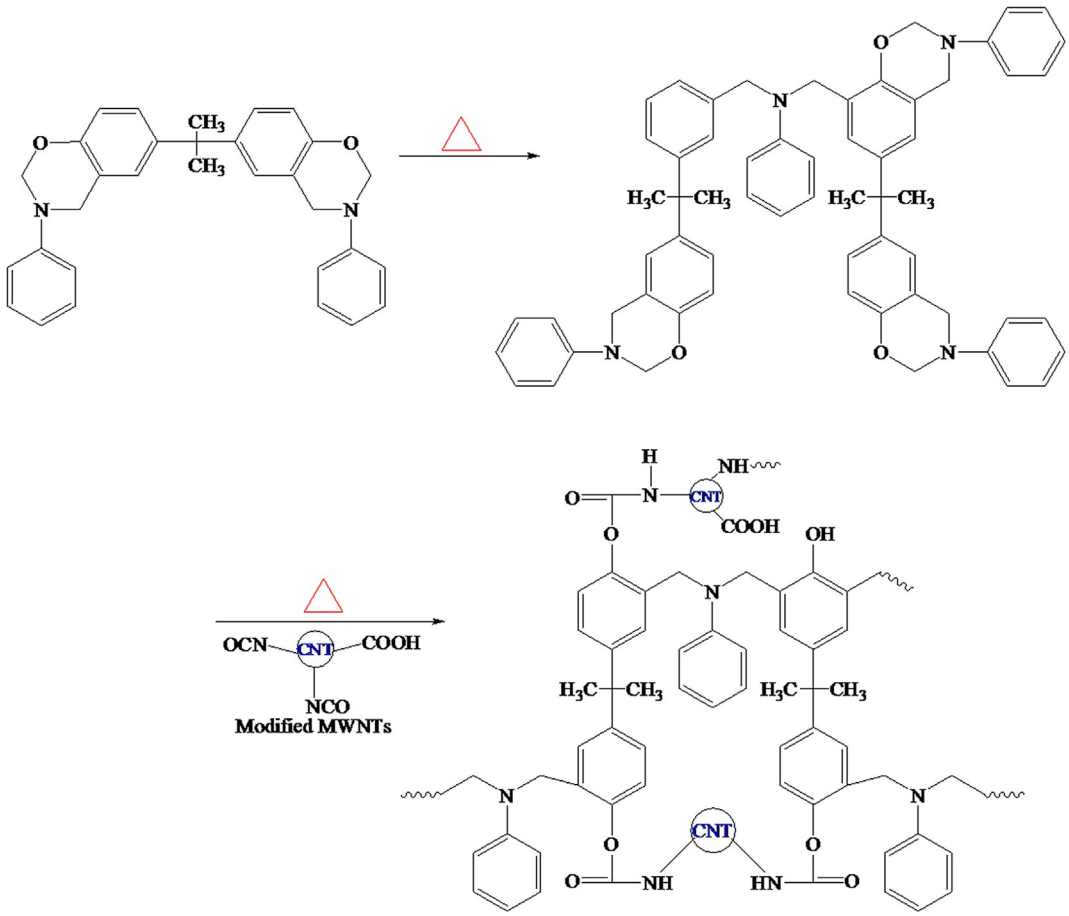

SCHEME 2 The possible curing reaction of BA-a monomer with the presence of modified MWCNT. *Reprinted with permission from Q. Chen, R.W. Xu, D. Yu. Multiwalled carbon nanotube/polybenzoxazine nanocomposites: preparation, characterization and properties, Polymer 47 (2006) 7711–7719.*

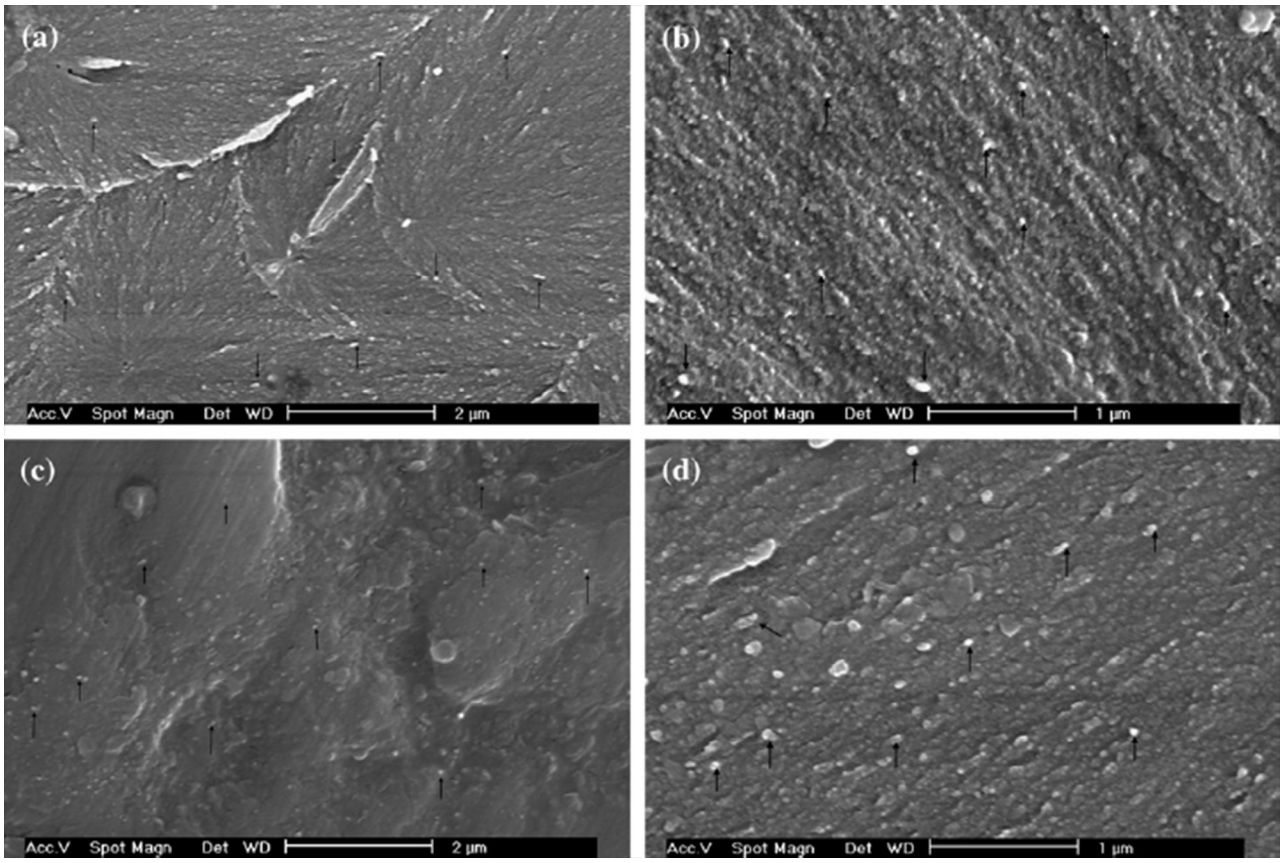

FIG. 1 SEM micrographs of the fracture surface of BA-a/MWCNT nanocomposites: (A) and (B) 1 wt% MWCNT; (C) and (D) 2 wt% MWCNT. *Reprinted with permission from Q. Chen, R.W. Xu, D. Yu. Multiwalled carbon nanotube/polybenzoxazine nanocomposites: preparation, characterization and properties, Polymer 47 (2006) 7711–7719.*

illustrates that the distribution of 1 wt% MWCNT was more homogeneous in the polybenzoxazine matrix than the one in 2 wt% MWCNT, where aggregation of MWCNT in polybenzoxazine matrix is possible.

The influence of MWCNT concentrations on the storage modulus (E') of poly(BA-a)/MWCNT nanocomposites was studied by dynamic mechanical analyzer (DMA). Adding 1 wt% MWCNT to polybenzoxazine increased the storage modulus because of the dispersion of the MWCNT in the polymer matrix. However, the storage modulus decreased for 2 wt% MWCNT into a polybenzoxazine matrix because of the aggregation of MWCNT. Interestingly, the glass-transition temperatures (T_g) of poly(BA-a)/MWCNT nanocomposites increased with increasing MWCNT concentrations because of the nano-reinforcement effect of MWCNT, restricting the motion of the polymer chain. Similarly, the T_g of poly (BA-a)/MWCNT nanocomposites decreased with higher concentrations of MWCNT because of the aggregation of the MWCNT, and the concentration of the polymer molecules that were in contact with the CNT's surface decreased, thus the fraction of the polymer that increased the T_g decreased for the aggregated sample [40].

4.2 Properties of Polybenzoxazine-Epoxy-CNT Nanocomposites

Alagar et al. studied the polybenzoxazine-epoxy-MWCNT nanocomposites, which were prepared via the reaction of 1,1-bis(3-methyl-4-hydroxyphenyl)cyclohexane, paraformaldehyde, and 4,4-diaminodiphenylmethane (BHC-ddm) as well as the reaction of *N*-(4-hydroxyphenyl)maleimide, 4, 4-diaminodiphenylmethane, and paraformaldehyde (BHM-ddm). They found that the tensile strength and flexural strength were increased by adding MWCNT. In addition, the strong interaction between benzoxazine-modified epoxy and MWCNT-reinforced systems led to increased T_g based on differential scanning calorimeter (DSC) analyses. According to thermogravimetric analyzer (TGA) analyses, blending 10 wt % benzoxazine with MWCNT-reinforced epoxy led to improved flame retardance (a high limiting oxygen index) and enhanced thermal stability. TEM micrographs of MWCNT-reinforced benzoxazine-modified (BHC-ddm and BHM-ddm) diglycidyl ether of bisphenol (DGEBA) epoxy nanocomposites showed self-nanoaggregations of MWCNT in the polymer matrix and in the hybrid nanocomposites, which looked like the dark sections shown in Fig. 2 [42].

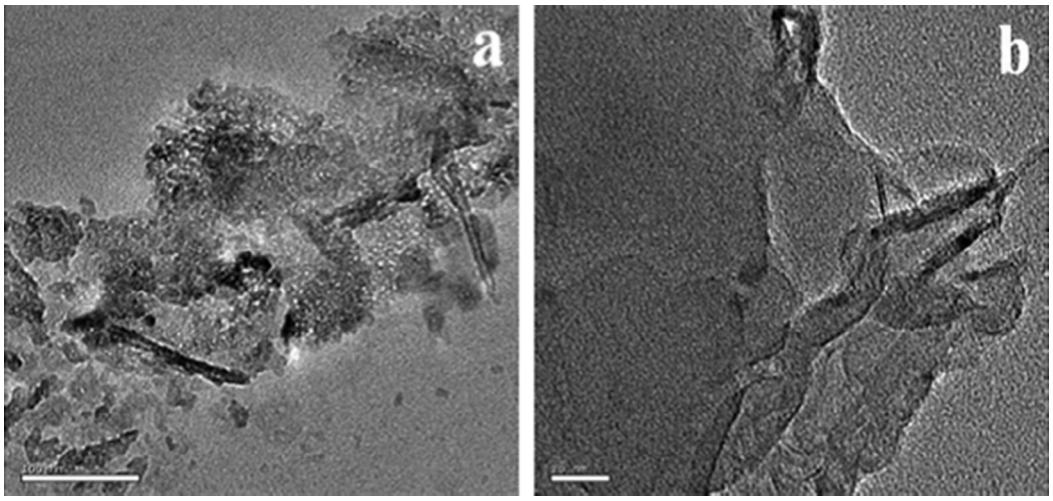

FIG. 2 TEM images of dispersion of (A) 0.5 wt% MWCNT in 10 wt% BHC-ddm-modified DGEBA epoxy nanocomposites, and (B) 0.5 wt% MWCNT in 10 wt% BHM-ddm-modified DGEBA epoxy nanocomposites. *Reprinted with permission from C.K. Chozhan, A. Chandramohan, M. Alagar. Influence of multiwalled carbon nanotubes on mechanical, thermal and electrical behavior of polybenzoxazine-epoxy nanocomposites, Polym. Plast. Technol. Eng. 54 (2015) 68–80.*

4.3 Properties of BA-fa and Poly(BA-fa)-Functionalized MWCNT Nanocomposites Through Diels-Alder Reaction

Liu et al. prepared benzoxazine monomer-functionalized MWCNTs that could self-polymerize or copolymerize with benzoxazine and maleimide compounds to afford bis (3-furfuryl-3,4-dihydro-2H-1,3-benzoxazinyl)isopropane (BA-fa) and poly(BA-fa) after a Diels-Alder reaction with bismaleimide and MWCNT (MWCNTs-poly(BA-fa), as shown in Scheme 3 [43]. Fig. 3 shows the TEM micrographs of MWCNT-(BA-fa), MWCNT-poly(BA-fa), and pristine MWCNT, indicating that the outer surfaces of the MWCNT are covered with amorphous layers of their organic portions with a thickness of c.3 nm. The thickness and performance of the retro-Diels-Alder reaction (the DA-adduct linkages between MWCNT and BA-fa in MWCNT-(BA-fa) could break down through the thermally induced retro-DA reaction) and the defunctionalization of MWCNT-(BA-fa) were investigated by FTIR analysis. As shown in Fig. 4, the disappearance of the absorption bands of MWCNT-(BA-fa) after heat treatment was observed, indicating the occurrence of a retro-DA reaction and the removal of (BA-fa) groups from the MWCNT-(BA-fa). As a result, the MWCNT-(BA-fa) became insoluble in *N*-methylpyrrolidone after a retro-DA reaction, as shown in Fig. 4B. Raman spectroscopy confirmed the benzoxazine-functionalized MWCNT nanohybrids. The characteristic tangential bands (G-bands) and a disorder band (D-band) are centered at 1588 cm^{-1} and 1333 cm^{-1}, respectively, for pure MWCNTs. The absorption intensities of the D-band confirmed the occurrence of covalent reactions between MWCNTs and the benzoxazine monomer. The addition of 0.5 and 1.5 wt% of functionalized MWCNTs in the polybenzoxazine matrix showed dispersion and no agglomeration of MWCNTs based on the TEM image. In 2013, based on dielectric constants and thermogravimetric analysis, Alagar et al. demonstrated that dielectric constants and the thermal stability of CNT-BS/BA-a increase along with increasing weight ratios of CNT modified with benzoxazine-functionalized silane (abbreviated as PH-pesa), which was prepared through the reaction of phenol, 3-aminopropyltriethoxysilane and paraformaldehyde [44].

5 PREPARATION OF POLYBENZOXAZINE-CNT THROUGH NONCOVALENT INTERACTION

There are many types of noncovalent interactions, including van der Waals forces, electrostatic, hydrophobic-hydrophobic, hydrogen bonding, and π-π stacking interactions. Here we report on several examples for dispersion of CNTs in a polybenzoxazine matrix by adsorption or by the incorporation of polynuclear aromatic compounds (eg, pyrene, porphyrin) into benzoxazine monomers, leading to π-π stacking interactions between pyrene units and CNTs. This approach did not affect the CNT structure, and as such did not lead to changes in the electronic properties. In this part of the chapter, we mainly investigate three kinds of synthesized benzoxazines.

5.1 Synthesis and Properties of Poly(PH-py)/SWCNT Nanocomposites

We synthesized a new class of pyrene-functional benzoxazines (P-py) through a Mannich condensation reaction

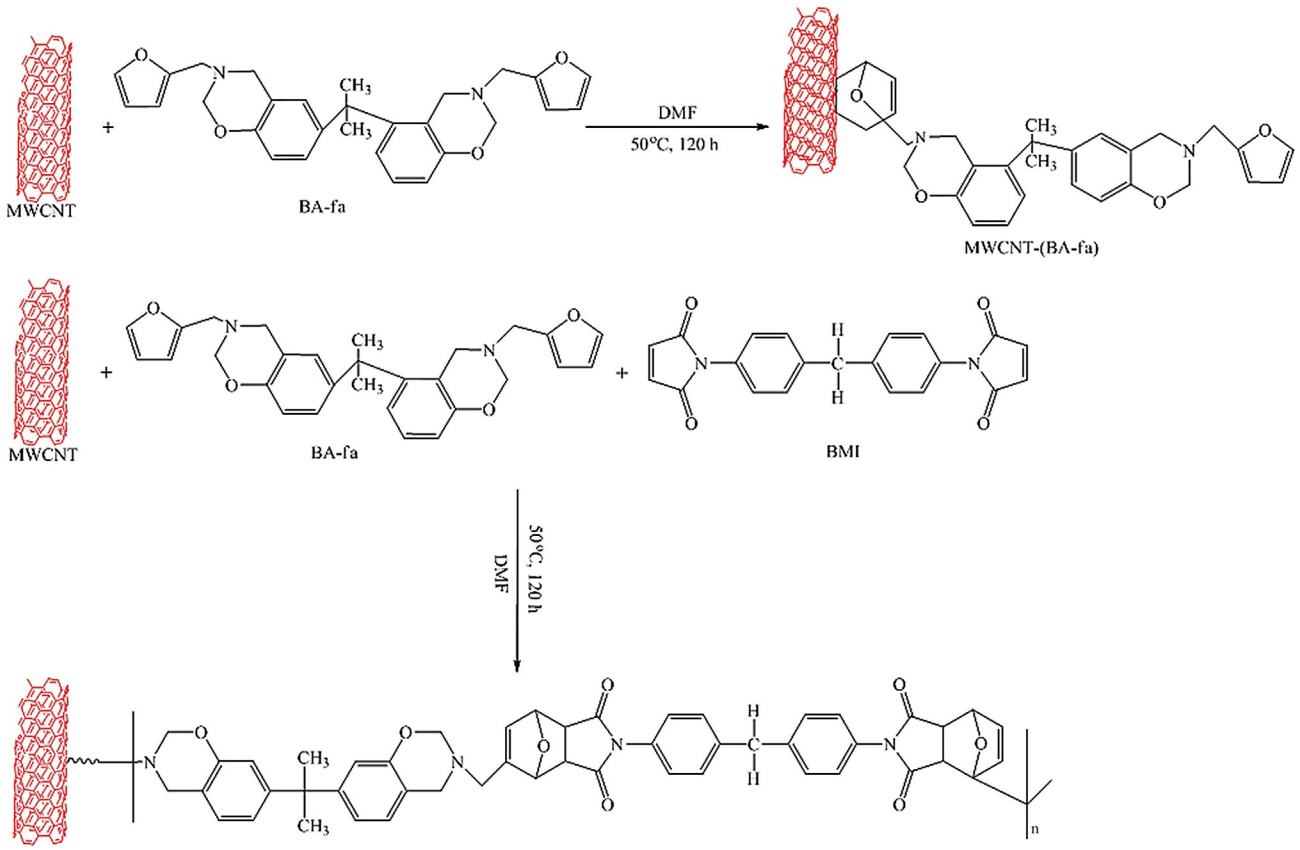

SCHEME 3 Preparation of MWCNTs functionalized with benzoxazine containing BA-fa and poly(BA-fa) through Diels-Alder reaction. *Reprinted with permission from Y.H. Wang, C.M. Chang, Y.L. Liu. Benzoxazine-functionalized multi-walled carbon nanotubes for preparation of electrically-conductive polybenzoxazines, Polymer 53 (2012) 106–112.*

between phenol, paraformaldehyde, and 1-aminopyrene in toluene-ethanol mixture, as shown in Scheme 4A [45]. Then we investigated the polymerization of P-py/SWCNTs nanocomposites before and after thermal curing and dispersion of CNTs inside the poly(P-py) matrix, as depicted in Scheme 4B. We performed TEM and photoluminescence spectroscopic analyses to investigate the interaction between pyrene moieties and SWCNTs through π-π stacking. As shown in Fig. 5, the dispersion of SWCNTs in a tetrahydrofuran (THF) solution with P-py as a clear brown solution was observed and was maintained for seven days, indicating that soluble hybrid complex nanocomposites were formed. The uniform dispersion of the SWCNTs within a P-py matrix without aggregation or clusters of SWCNTs was studied by TEM, as shown in Fig. 5. In addition, after the formation of a P-py/SWNCTs hybrid complex, the emission intensity of pyrene was quenched, which is ascribed to the π-π stacking interaction.

The thermal behavior of the P-py/SWCNT's hybrid complex was measured by DSC. Fig. 6 shows that both curing temperature and enthalpy decreased with the increase of the SWCNT's content, because of the CNT's ability to act as the catalyst and also hinder the mobility of the polymer chain to decrease the cross-linking reaction of polybenzoxazines after ring-opening. Also, we investigated the effect of various amounts of SWCNTs on the T_g of poly(P-py) by DSC and DMA analyses. The results indicated that the T_g of poly(P-py) increased with the increase of SWCNT contents at lower than 3 wt%. On the other hand, the decreased T_g of 5 wt% SWCNTs was attributed to the decrease in the cross-linking density of the nanocomposites. DMA analyses indicated that the T_g of pure poly(P-py) and the poly(P-py)/SWCNT (3 wt%) hybrid after curing are 130°C and 156°C, respectively. Interestingly, based on the TGA results, blending 5 wt% of SWCNT content with P-py and its thermal polymerization, the values of thermal degradation temperature (T_d) and char yield of the poly(P-py)/SWCNTs nanocomposites increased, which blocked the premature evaporation of the decomposed molecular fragments via CNTs.

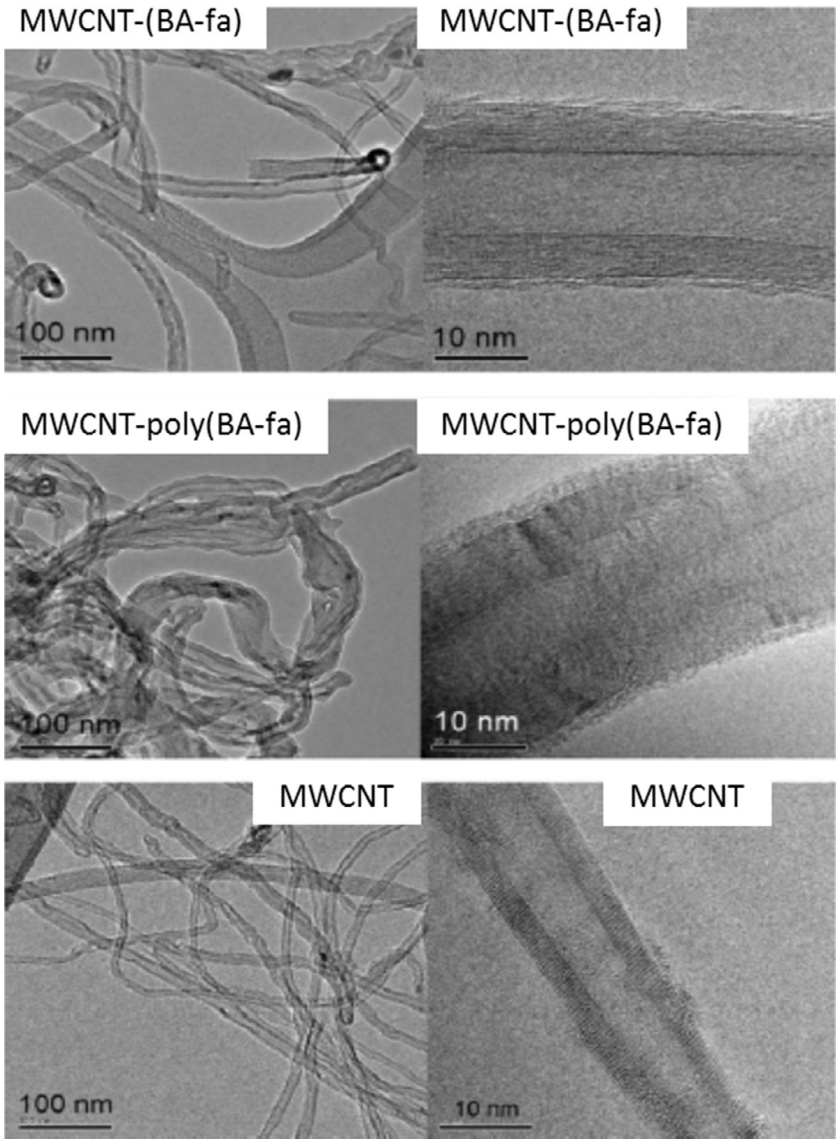

FIG. 3 TEM images of MWCNT-(BA-fa), MWCNT-poly(BA-fa), and MWCNT. *Reprinted with permission from Y.H. Wang, C.M. Chang, Y.L. Liu. Benzoxazine-functionalized multi-walled carbon nanotubes for preparation of electrically-conductive polybenzoxazines, Polymer 53 (2012) 106–112.*

5.2 Synthesis and Properties of Poly (COH-py) and Poly(DI-COH-py)/SWCNT Nanocomposites

We also designed a new class of multifunctional benzoxazine monomer containing coumarin units as photoresponsive material and pyrene as π-π stacking through Mannich condensation of 4-methyl-7-hydroxycoumarin, paraformaldehyde, and 1-aminopyrene in 1,4-dioxane (COH-py) and after photodimerization of the coumarin units through [2π+2π] cycloaddition (abbreviated as DI-COH-py), as shown in Scheme 5 [46–48]. Then we prepared poly(COH-py) and poly(DI-COH-py)/SWCNT nanocomposites. Similarly, the emission intensity of poly(COH-py) decreased or reduced after the resin was blended with the SWCNTs. The TEM image shows that the dispersion of SWCNTs was homogeneous, without any aggregation, and less entangled in the poly(COH-py) matrix.

DSC and TGA analyses were used to examine the characteristics of poly(COH-py) and poly(COH-py)/SWCNT nanocomposites after thermal curing. Because of lower cross-linking densities after blending poly(COH-py) with different SWCNTs contents (1, 3, and 5 wt%), the T_g of nanocomposites decreased compared to that of poly(COH-py). DSC analysis showed increased T_g of pure poly(DI-COH-py). Furthermore, the T_g (205°C) of poly(DI-COH-py)/SWCNT (3 wt%) was even higher than those (200°C) of pure poly(COH-py) and poly(COH-py)/SWCNT (3 wt%), which

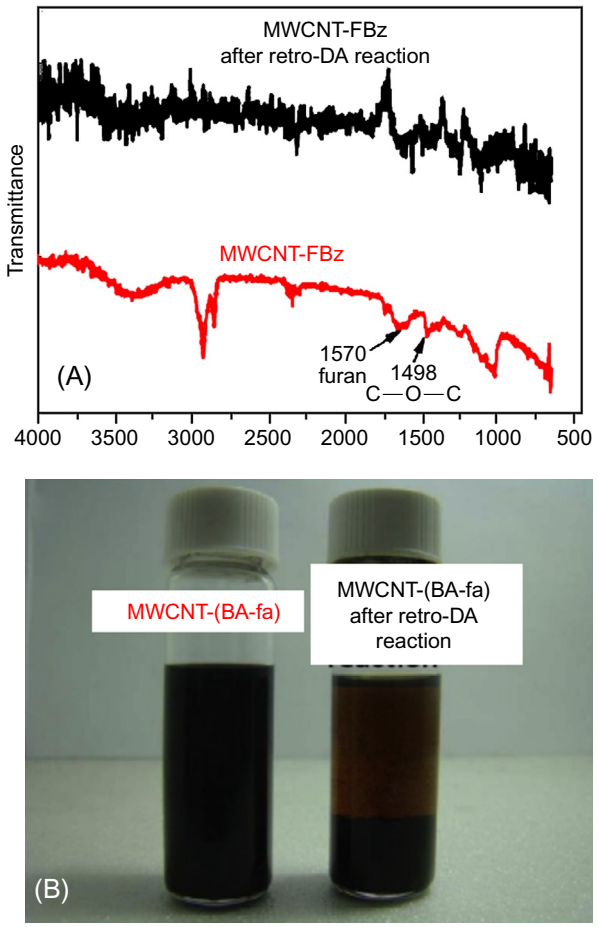

FIG. 4 (A) FTIR spectra of MWCNT-(BA-fa) and after retro-DA reaction, and (B) photographs of MWCNT-(BA-fa) after retro-DA reaction. *Reprinted with permission from Y.H. Wang, C.M. Chang, Y.L. Liu. Benzoxazine-functionalized multi-walled carbon nanotubes for preparation of electrically-conductive polybenzoxazines, Polymer 53 (2012) 106–112.*

was attributed to an increase in the cross-linking density after photodimerization of the coumarin moieties. Fig. 7 shows that the T_d and char yield of poly(DI-COH-py)/SWCNT (3 wt%) are greater when compared to the coumarin containing polybenzoxazine without UV irradiation, which caused an increase in the cross-linking density and the nano-reinforcement effect.

5.3 Synthesis and Properties of Poly(Azo-COOH-py)/CNT Nanocomposites

We also prepared a new trifunctional Azo-COOH-py that contained a azobenzene group, a carboxylic acid unit, and pyrene moiety via the condensation reaction between Azo-COOH, 1-aminopyrene, and paraformaldehyde, which enhanced the formation of highly dispersible Azo-COOH-py/CNT nanocomposites through π-π stacking interactions of pyrene and CNT units, as shown in Scheme 6 [49]. As shown in the TEM image (Fig. 8), both SWCNTs and MWCNTs could be dispersed in the Azo-COOH-Py benzoxazine matrix before and after thermal curing. The DSC thermogram showed that the maximum exothermic peak for oxazine ring-opening of the Azo-COOH-py monomer shifted to a lower temperature in the presence of SWCNTs, compared to poly(Azo-COOH-py), which was attributed to the presence of the carboxyl group and the catalytic effect of SWCNTs. More interestingly in this study, SWCNTs acted as stronger catalysts to initiate ring-opening of the oxazine ring than MWCNTs did and also increased the enthalpy of polymerization for SWCNTs. In order to compare the effect of the SWCNTs and MWCNTs on the thermal stability of Azo-COOH-py after thermal polymerization, the thermal stability was monitored by TGA analyses. Fig. 9 shows that the presence of SWCNTs increased the char yield and the T_d of poly(Azo-COOH-py) more than those in the presence of MWCNTs, probably because the SWCNTs had a greater thermal conductivity than the SWCNTs in the polybenzoxazine matrix.

5.4 Synthesis and Properties of Poly(BA-a) and Poly(MDP-a)/MWCNT Nanocomposites

Doubis et al. designed and synthesized two different kinds of benzoxazine monomers, BA-a and MDP-a (methyl-4,4-bis-[6-(3-phenyl-3,4-dihydro-2H-1,3-benzoxazine)]pentanoate), through a Mannich reaction, and then they blended the resins with different MWCNT concentrations to afford polybenzoxazine/MWCNT nanocomposites [50]. They investigated the dispersion of MWCNTs in both benzoxazine resins via a rheological approach, revealing the enhancement of network connectivity through the interaction of the MWCNT particles based on rubbery plateau measurements. DSC analysis showed that both monomers with MWCNT contents had a single curing temperature with a slight shift to lower a temperature, as compared to the exothermic peak of pure benzoxazine monomers, because of the improvement in the thermal conductivity of the system via MWCNTs. Furthermore, the addition of MWNCTs improved the T_d and char yield for both benzoxazine monomers based on TGA analysis under N_2 and air atmospheres. Doubis et al. also synthesized a P-dmm benzoxazine monomer through a Mannich reaction of 1, 4-phenylene diamine, phenol, and paraformaldehyde (abbreviated as PH-dmm) [51]. Poly(PH-dmm)/MWCNTs exhibited excellent thermomechanical stability, a higher T_d, and strong natural interactions with CNTs. In 2013 Doubis et al. synthesized two kinds of benzoxazine monomers, BA-a and P-dmm. They observed that the thermomechanical behavior of poly(P-dmm)/0.5 wt% MWCNTs was much higher than that of poly(BA-a)/0.5 wt%

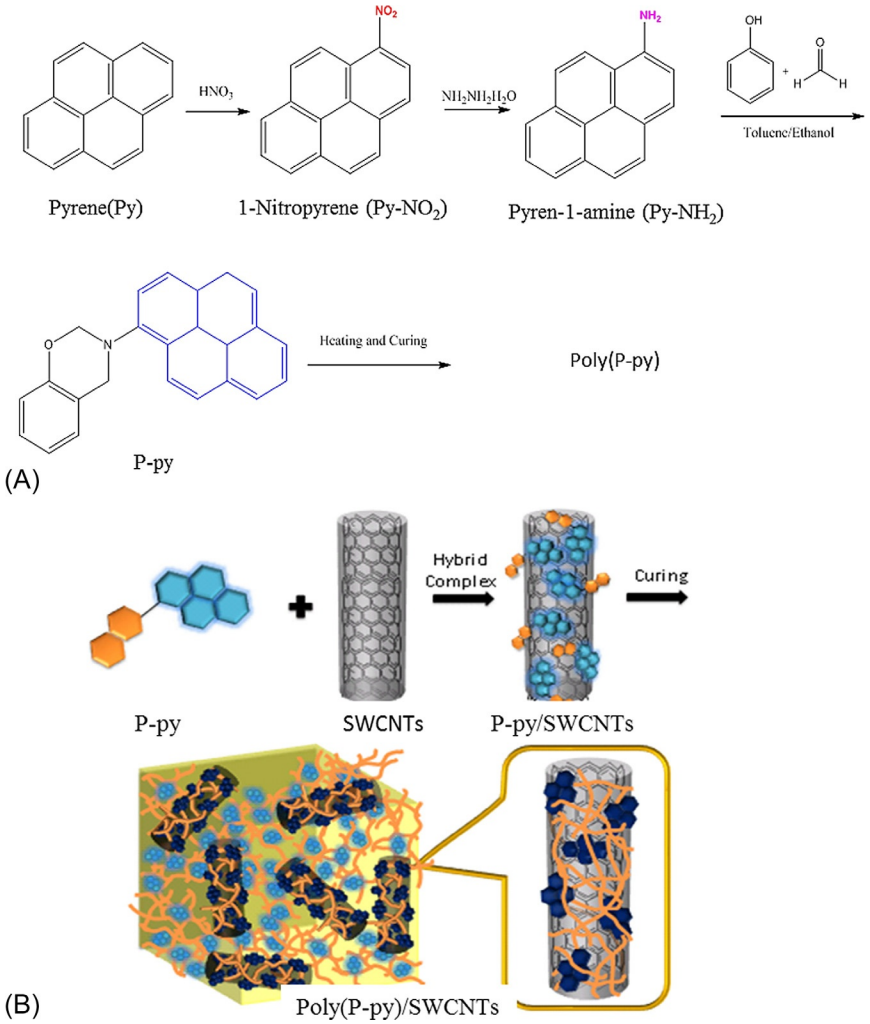

SCHEME 4 (A) The synthesis of P-py monomer and (B) proposed the formation of poly(P-py)/SWCNT hybrid complexes, stabilized through a π-π stacking interaction. *Reprinted with permission from C.C. Yang, Y.C. Lin, P.I. Wang, D.J. Liaw, S.W. Kuo. Polybenzoxazine/single-walled carbon nanotube nanocomposites stabilized through noncovalent bonding interactions, Polymer 55 (2014) 2044–2050.*

MWCNTs, based on the thermomechanical profile. Additionally, both polybenzoxazine's nanocomposite matrices showed a uniform and random dispersion with small clusters, as presented in TEM images [52]. Chapartequi et al. also successfully fabricated MWCNT buckypaper/benzoxazine nanocomposites (abbreviated as BA-a modified with diglycidyl ether [DGEBBA] epoxy). This system showed that, based on electrical conductivity analysis, the electrical conductivity values are much higher than those of traditional CNT/polymer nanocomposites, and they also exhibited a higher glass-transition temperature [53].

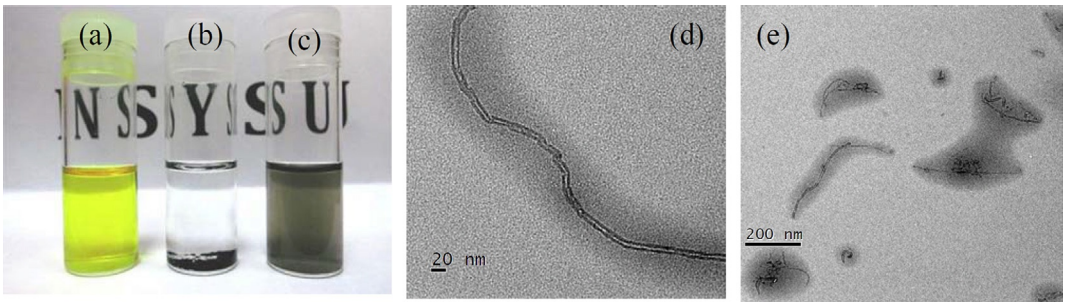

FIG. 5 Photograph of (A) pure PH-py; (B) SWCNT; (C) P-py/SWCNT nanocomposites in tetrahydrofuran (THF) solution; and (D, E) TEM image of sample after thermal curing. *Reprinted with permission from C.C. Yang, Y.C. Lin, P.I. Wang, D.J. Liaw, S.W. Kuo. Polybenzoxazine/single-walled carbon nanotube nanocomposites stabilized through noncovalent bonding interactions, Polymer 55 (2014) 2044–2050.*

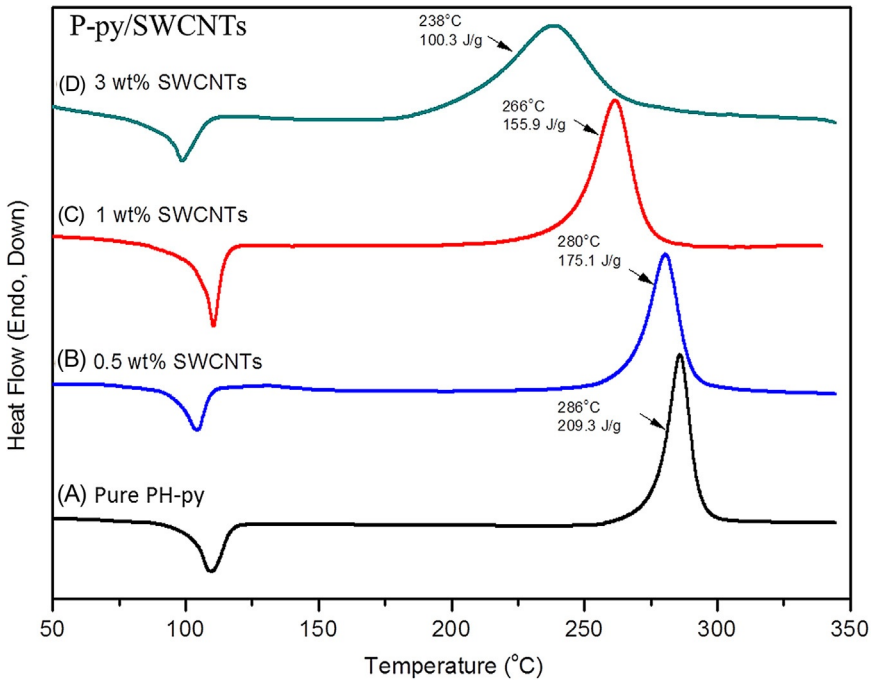

FIG. 6 DSC profile of the thermal curing behavior of P-py mixtures with various SWCNT contents. *Reprinted with permission from C.C. Yang, Y.C. Lin, P.I. Wang, D.J. Liaw, S.W. Kuo. Polybenzoxazine/single-walled carbon nanotube nanocomposites stabilized through noncovalent bonding interactions, Polymer 55 (2014) 2044–2050.*

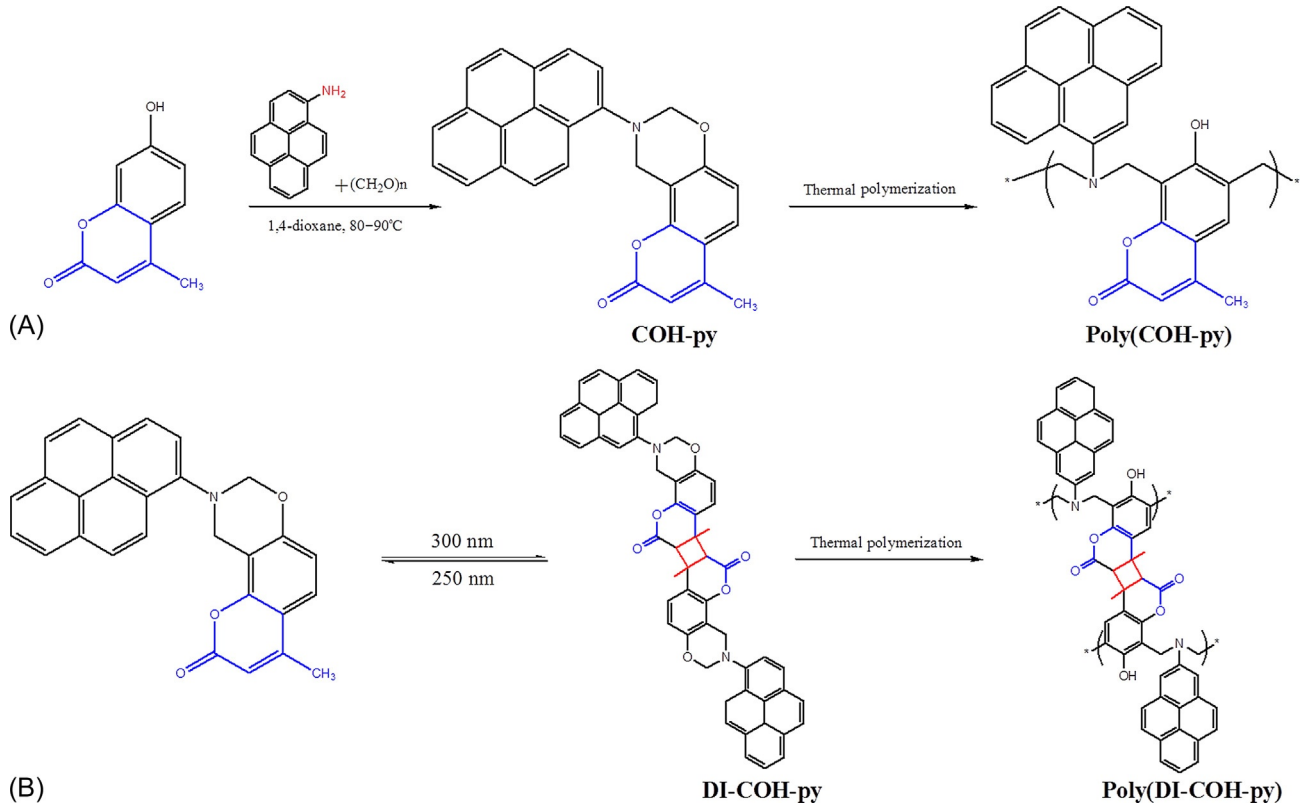

SCHEME 5 (A) Synthesis and chemical structures of COH-py and poly(COH-py) and (B) photodimerization of COH-py and subsequent thermal curing to form poly(DI-COH-py). *Reprinted with permission from M.G. Mohamed, K.C. Hsu, S.W. Kuo. Bifunctional polybenzoxazine nanocomposites containing photo-crosslinkable coumarin units and pyrene units capable of dispersing single-walled carbon nanotubes, Polym. Chem. 6 (2015) 2423–2433.*

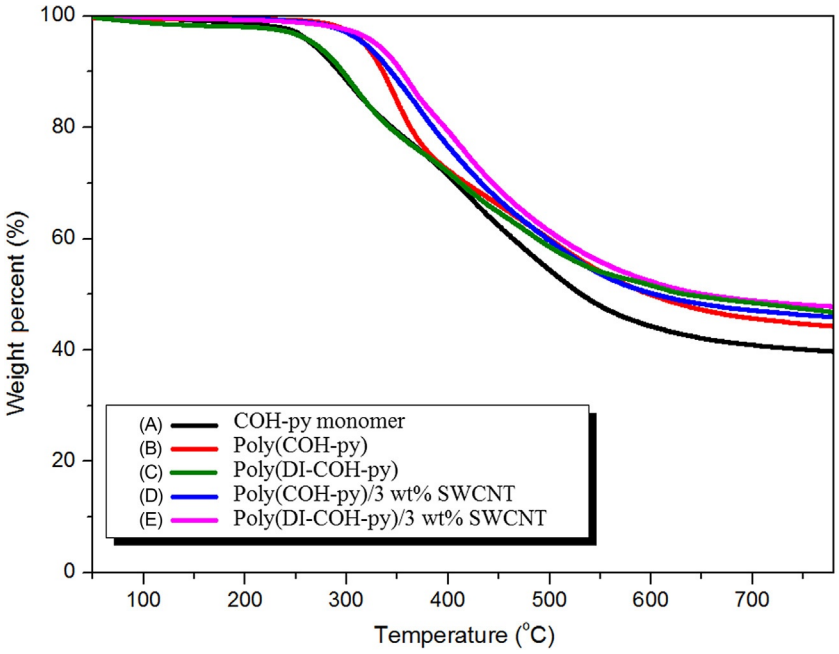

FIG. 7 TGA analyses of (A) COH-py monomer, (B) poly(COH-py), (C) poly(DI-COH-py), (D) poly(COH-py)/SWCNT (3 wt%), and (E) poly- (DI-COH-py)/SWCNT (3 wt%). *Reprinted with permission from M.G. Mohamed, K.C. Hsu, S.W. Kuo. Bifunctional polybenzoxazine nanocomposites containing photo-crosslinkable coumarin units and pyrene units capable of dispersing single-walled carbon nanotubes, Polym. Chem. 6 (2015) 2423–2433.*

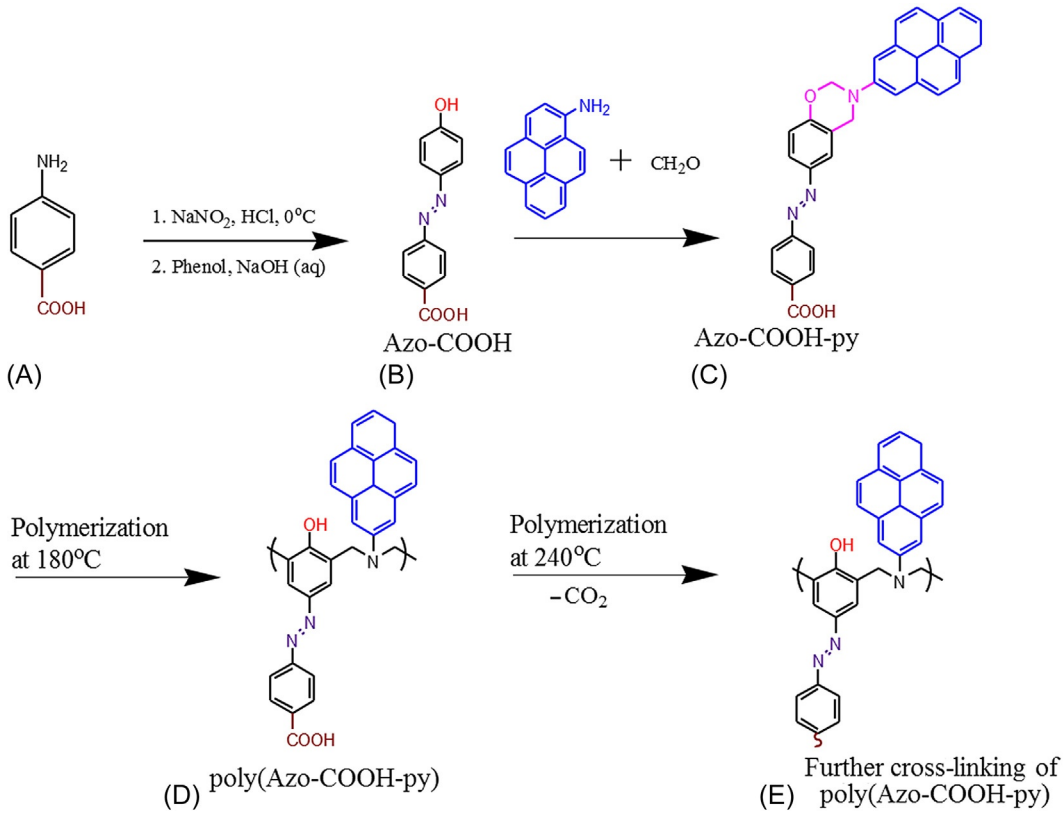

SCHEME 6 Chemical structure of (A) 4-aminobenzoic acid and synthesis of (B) Azo-COOH, (C) Azo-COOH-py, (D) poly(Azo-COOH-py), and (E) further cross-linking of poly(Azo-COOH-py). *Reprinted with permission from M.G. Mohamed, C.H. Hsiao, F. Luo, L. Dai, S.W. Kuo, Multifunctional polybenzoxazine nanocomposites containing photoresponsive azobenzene units, catalytic carboxylic acid groups, and pyrene units capable of dispersing carbon nanotubes, RSC Adv. 5 (2015) 45201–45212.*

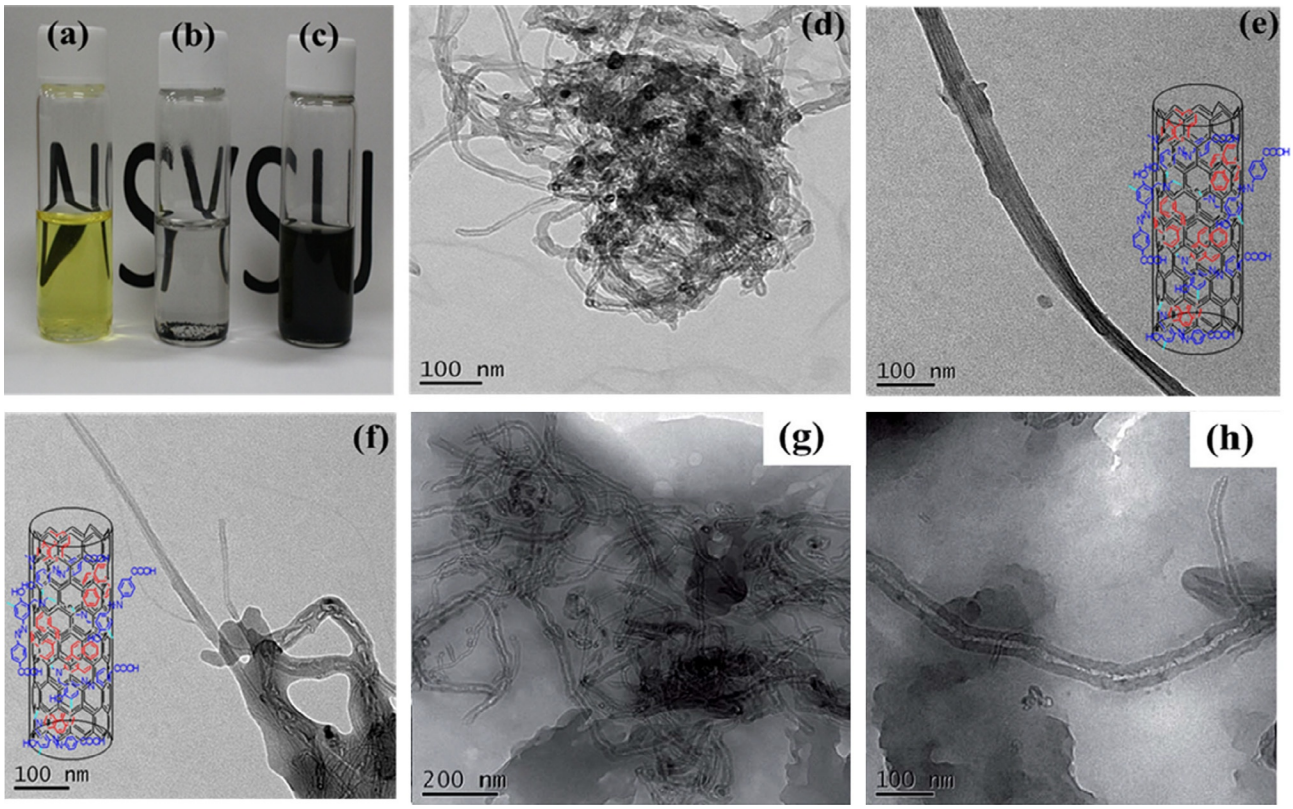

FIG. 8 (A–C) Photographs of (A) Azo-COOH-py, (B) pristine SWCNTs, and (C) Azo-COOH-py/SWCNTs (5 wt%) in THF; (D–H) TEM images of (D) pure SWCNTs, (E and F) Azo-COOH-py/SWCNTs (5 wt%), (E) before and (F) after thermal curing; and (G and H) Azo-COOH-py/MWCNTs (5 wt%), (G) before and (H) after thermal curing. *Reprinted with permission from M.G. Mohamed, C.H. Hsiao, F. Luo, L. Dai, S.W. Kuo, Multifunctional polybenzoxazine nanocomposites containing photoresponsive azobenzene units, catalytic carboxylic acid groups, and pyrene units capable of dispersing carbon nanotubes, RSC Adv. 5 (2015) 45201–45212.*

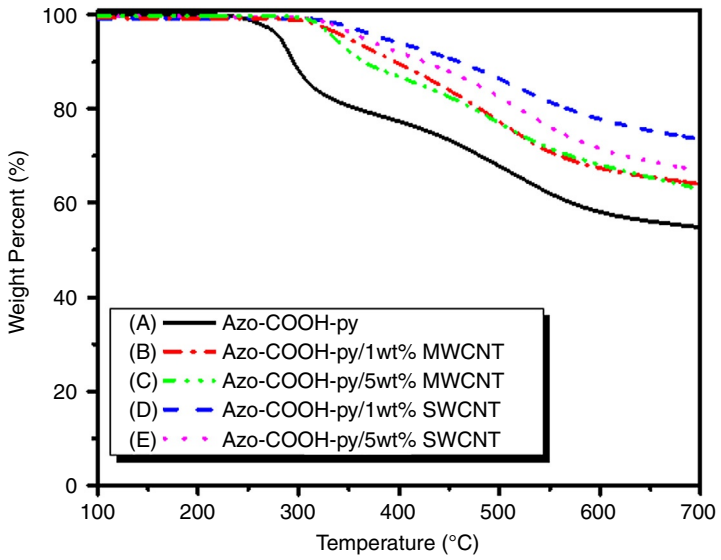

FIG. 9 TGA analyses of (A) Azo-COOH-py and (B–E) its nanocomposites with (B) 1 wt% MWCNTs, (C) 5 wt% MWCNTs, (D) 1 wt% SWCNTs, and (E) 5 wt% SWCNTs after thermal curing. *Reprinted with permission from M.G. Mohamed, C.H. Hsiao, F. Luo, L. Dai, S.W. Kuo, Multifunctional polybenzoxazine nanocomposites containing photoresponsive azobenzene units, catalytic carboxylic acid groups, and pyrene units capable of dispersing carbon nanotubes, RSC Adv. 5 (2015) 45201–45212.*

6 CONCLUSION

Cylindrical CNTs' structure possesses unusual properties, such as high electrical conductivity and excellent mechanical properties, which are valuable for many applications, including the nanotechnology, optics, supercapacitor, paper batteries, and solar cell industries. In this chapter, we explained the two methods used for modifying and enhancing the dispersion of CNTs in a polybenzoxazine matrix through covalent bonding and noncovalent interactions. The modification of MWCNTs by chemical reaction with nitric acid combined with a large amount of TDI was achieved. This chemical reaction increased the concentration of carboxyl groups, COOH, on the CNTs' surfaces, which can act as a catalyst for accelerating the ring-opening polymerization of benzoxazine. Furthermore, the isocyanate units can react with the phenolic hydroxyl groups, which are generated as a result of polymerization of the benzoxazine monomer. The formation of such interfacial covalent bonding improved the uniform dispersion of CNTs through the adhesion force between the polybenzoxazine matrix and the MWCNTs. The poly(BA-a)/MWCNT nanocomposites showed good dispersion and a high glass-transition temperature based on dynamic mechanical analysis. The glass-transition temperature of the poly(BA-a)/MWCNT nanocomposites decreased as concentrations of the MWCNTs' contents increased, which is explained by the aggregation of MWCNTs in the polybenzoxazine matrix. Functionalization of MWCNTs by nitric acid changed the chemical structure of the MWCNTs from sp^2 to sp^3 hybridization and led to a loss of the unique electrical and mechanical properties. We used a noncovalent interaction (π-π stacking interaction) to prepare polybenzoxazines/CNT nanocomposites via the interaction between pyrene units and the CNTs without changing the hybridization of carbon atoms from sp^2 to sp^3 and influencing the electrical properties of the CNT. Interestingly, (1) three kinds of polybenzoxazine/CNT nanocomposites displayed a uniform dispersion of CNTs in those matrices before and after the thermal curing lowered the curing temperature and increased the glass-transition temperature, which is attributed to an increase in the cross-linking density; and (2) SWCNTs can act as effective catalysts to accelerate ring-opening polymerization of benzoxazine better than MWCNTs can.

REFERENCES

[1] M. Ouyang, J.L. Huang, C.L. Cheung, C.M. Lieber, Atomically resolved single-walled carbon nanotube intramolecular junctions, Science 291 (2001) 97–100.

[2] H.W. Kroto, J.R. Heath, S.C. O'BRIEN, R.F. Curl, R.E. Smalley, C60: bukminsterfullerene, Nature 318 (1985) 162–163.

[3] L. Chico, V.H. Crespi, L.X. Benedict, S.G. Louie, M.L. Cohen, Pure carbon nanoscale devices: nanotube heterojunctions, Phys. Rev. Lett. 76 (1996) 971–974.

[4] R.H. Baughman, A.A. Zakhidov, W.A. de Heer, Carbon nanotubes—the route toward applications, Science 297 (2002) 787–792.

[5] S. Iijima, T. Ichihashi, Single-shell carbon nanotubes of 1 nm diameter, Nature 363 (1993) 603–605.

[6] J. Cao, Q. Wang, M. Rolandi, H. Dai, Aharonov–Bohm interference and beating in single-walled carbon-nanotube interferometers, Phys. Rev. Lett. 93 (2004) 1–4.

[7] W. Yang, P. Thordarson, J.J. Gooding, S.P. Ringer, F. Braet, Carbon nanotubes for biological and biomedical applications, Nanotechnology 18 (2007) 412001–412013.

[8] J.L. Bahr, J.M. Tour, Covalent chemistry of single-wall carbon nanotubes, J. Mater. Chem. 12 (2002) 1952–1958.

[9] A. Hirsch, Functionalization of single-walled carbon nanotubes, Angew. Chem. Int. Ed. 41 (2002) 1853–1859.

[10] E. Abbasi, A.S. Fekri, A. Abolfazl, M. Morteza, N.H. Tayefi, H. Younes, N.-K. Kazem, P.-A. Roghiyeh, Dendrimers: synthesis, applications, and properties, Nanoscale Res. Lett. 9 (2014) 247–255.

[11] M.J. Yacaman, M.M. Yoshida, L. Rendon, J.G. Santiesteban, Catalytic growth of carbon microtubules with fullerene structure, Appl. Phys. Lett. 62 (1993) 202–204.

[12] S. Iijima, Helical microtubules of graphitic carbon, Nature 354 (1991) 56–58.

[13] R. Hirlekar, M. Yamagar, H. Garse, M. Vij, V. Kadam, Carbon nanotubes and its applications: a review, Asian J. Pharm. Clin. Res. 2 (2009) 17–27.

[14] P.X. Hou, S. Bai, Q.H. Yang, C. Liu, H.M. Cheng, Multi-step purification of carbon nanotubes, Carbon 40 (2002) 81–85.

[15] B.Q. Wei, R. Vajtai, P.M. Ajayan, Reliability and current carrying capacity of carbon nanotubes, Appl. Phys. Lett. 79 (2001) 1172–1174.

[16] M.J. O'Connell, S.M. Bachilo, C.B. Huffman, V.C. Moore, M.S. Strano, E.H. Haroz, K.L. Rialon, P.J. Boul, W.H. Noon, C. Kittrell, J. Ma, R. H. Hauge, R.B. Weisman, R.E. Smalley, Band gap fluorescence from individual single-walled carbon nanotubes, Science 297 (2002) 593–596.

[17] T. Dürkop, B.M. Kim, M.S. Fuhrer, Properties and applications of high-mobility semiconducting nanotubes, J. Phys. Condens. Matter 16 (2004) R553–R580.

[18] T.W. Ebbesen, H.J. Lezec, H. Hiura, J.W. Bennett, H.F. Ghaemi, T. Thio, Electrical conductivity of individual carbon nanotubes, Nature 382 (1996) 54–56.

[19] M.M.J. Treacy, T.W. Ebbesen, J.M. Gibson, Exceptionally high Young's modulus observed for individual carbon nanotubes, Nature 381 (1996) 678–680.

[20] J.P. Salvetat, A.J. Kulik, J.M. Bonard, G.A.D. Briggs, T. Stockli, K. Metenier, L. Forró, Elastic modulus of ordered and disordered multiwalled carbon nanotubes, Adv. Mater. 11 (1999) 161–165.

[21] J.P. Salvetat, J.M. Bonard, N.H. Thomson, A.J. Kulik, L. Forró, W. Benoit, L. Zhppiroli, Mechanical properties of carbon nanotubes, Appl. Phys. A Mater. Sci. Process. 69 (1999) 255–260.

[22] M.F. Yu, B.S. Files, S. Arepalli, R.S. Ruoff, Tensile loading of ropes of single wall carbon nanotubes and their mechanical properties, Phys. Rev. Lett. 84 (2000) 5552–5555.

[23] T. Ozaki, Y. Iwasa, T. Mitani, Stiffness of single-walled carbon nanotube under large strain, Phys. Rev. Lett. 84 (2000) 1712–1716.
[24] J.P. Salvetat, G.A.D. Briggs, J.M. Bonard, R.R. Bacsa, A.J. Kulik, T. Stockli, L. Forró, Elastic and shear moduli of single-walled carbon nanotube ropes, Phys. Rev. Lett. 82 (1999) 944–947.
[25] J.P. Lu, Elastic properties of single and multilayered nanotubes, J. Phys. Chem. Solids 58 (1997) 1649–1652.
[26] A. Hirsch, Functionalization of single-walled carbon nanotubes, Angew. Chem. Int. Ed. 41 (2002) 1853–1859.
[27] M. Holzinger, O. Vostrowsky, A. Hirsch, F. Hennrich, M. Kappes, R. Weiss, F. Jellen, Sidewall functionalization of carbon nanotubes, Angew. Chem. Int. Ed. 40 (2001) 4002–4005.
[28] V.N. Khabashesku, W.E. Billups, J.L. Margrave, Fluorination of single-walled carbon nanotubes and subsequent derivatization reactions, Acc. Chem. Res. 35 (2002) 1087–1095.
[29] K. Balasubramanian, M. Burghard, Chemically functionalized carbon nanotubes, Small (2005) 180–192.
[30] C. Ehli, G.M.A. Rahman, N. Jux, D. Balbinot, D.M. Guldi, D.F. Paolucci, M. Marcaccio, D. Paolucci, M. Melle-Franco, F. Zerbetto, S. Campidelli, M. Prato, Interactions in single wall carbon nanotubes/pyrene/porphyrin nanohybrids, J. Am. Chem. Soc. 128 (2006) 11222–11231.
[31] A. Star, J.F. Stoddart, D. Steuerman, M. Diehl, A. Boukai, E.W. Wong, X. Yang, S.W. Chung, H. Choi, J.R. Heath, Preparation and properties of polymer wrapped single-walled carbon nanotubes, Angew. Chem. Int. Ed. 40 (2001) 1721–1725.
[32] A. Star, Y. Liu, K. Grant, L. Ridvan, J.F. Stoddart, D.W. Steuerman, M.R. Diehl, A. Boukai, J.R. Heath, Noncovalent side-wall functionalization of single walled carbon nanotubes, Macromolecules 36 (2003) 553–560.
[33] Y.L. Zhao, L. Hu, J.F. Stoddart, G. Gruner, Pyrene cyclodextrin-decorated single walled carbon nanotube field-effect transistors as chemical sensors, Adv. Mater. 20 (2008) 1910–1915.
[34] X. Lou, C. Detrembleur, V. Sciannamea, C. Pagnoulle, R. Jerome, Grafting of alkoxtamine end-capped (co)polymers onto multi-walled carbon nanotubes, Polymer 45 (2004) 6097–6102.
[35] K. Fu, W. Huang, Y. Lin, L.A. Riddle, D.L. Carroll, Y.P. Sun, Defunctionalization of functionalized carbon nanotubes, Nano Lett. 1 (2001) 439–441.
[36] Y.X. Wang, H. Ishida, Development of low-viscosity benzoxazine resins and their polymers, J. Appl. Polym. Sci. 86 (2002) 2953–2966.
[37] K. Zhang, H. Ishida, An anomalous trade-off effect on the properties of smart ortho-functional benzoxazines, Polym. Chem. 6 (2015) 2541–2550.
[38] K. Zhang, J. Liu, H. Ishida, An ultrahigh performance cross-linked polybenzoxazole via thermal conversion from poly(benzoxazine amic acid) based on smart o-benzoxazine chemistry, Macromolecules 47 (2014) 8671–8681.
[39] M.G. Mohamed, W.C. Su, Y.C. Lin, C.F. Wang, J.K. Chen, K.U. Jeong, S.W. Kuo, Azopyridine-functionalized benzoxazine with $Zn(ClO_4)_2$ form high-performance polybenzoxazine stabilized through metal–ligand coordination, RSC Adv. 4 (2014) 50373–50385.
[40] Q. Chen, R.W. Xu, D. Yu, Multiwalled carbon nanotube/polybenzoxazine nanocomposites: preparation, characterization and properties, Polymer 47 (2006) 7711–7719.
[41] R. Xu, P. Zhang, J. Wang, D. Yu, Polybenzoxazine-CNT nanocomposites, in: T. Agag, H. Ishida (Eds.), Handbook of Benzoxazine Resins, Elsevier, Amsterdam, 2011, , pp. 541–554.
[42] C.K. Chozhan, A. Chandramohan, M. Alagar, Influence of multi-walled carbon nanotubes on mechanical, thermal and electrical behavior of polybenzoxazine-epoxy nanocomposites, Polym. Plast. Technol. Eng. 54 (2015) 68–80.
[43] Y.H. Wang, C.M. Chang, Y.L. Liu, Benzoxazine-functionalized multi-walled carbon nanotubes for preparation of electrically-conductive polybenzoxazines, Polymer 53 (2012) 106–112.
[44] M. Selvia, M.R. Vengatesan, P. Prabunathan, J.K. Song, M. Alagar, High dielectric multiwalled carbon nanotube-polybenzoxazine nanocomposites for printed circuit board applications, Appl. Phys. Lett. 103 (2013) 152902–152905.
[45] C.C. Yang, Y.C. Lin, P.I. Wang, D.J. Liaw, S.W. Kuo, Polybenzoxazine/single-walled carbon nanotube nanocomposites stabilized through noncovalent bonding interactions, Polymer 55 (2014) 2044–2050.
[46] M.G. Mohamed, K.C. Hsu, S.W. Kuo, Bifunctional polybenzoxazine nanocomposites containing photo-crosslinkable coumarin units and pyrene units capable of dispersing single-walled carbon nanotubes, Polym. Chem. 6 (2015) 2423–2433.
[47] B. Kiskan, Y. Yagci, Thermally curable benzoxazine monomer with a photodimerizable coumarin group, J. Polym. Sci. A Polym. Chem. 45 (2007) 1670–1676.
[48] P. Froimowicz, C.R. Arza, S. Ohashi, H. Ishida, Tailor-made and chemically designed synthesis of coumarin-containing benzoxazines and their reactivity study toward their thermosets. J. Polym. Sci. A Polym. Chem. 54 (2016) 1428–1435, http://dx.doi.org/10.1002/pola.27994.
[49] M.G. Mohamed, C.H. Hsiao, F. Luo, L. Dai, S.W. Kuo, Multifunctional polybenzoxazine nanocomposites containing photoresponsive azobenzene units, catalytic carboxylic acid groups, and pyrene units capable of dispersing carbon nanotubes, RSC Adv. 5 (2015) 45201–45212.
[50] C. Zuniga, L. Bounaud, G. Ligadas, J.C. Ronda, M. Galià, V. Cadiz, P. Dubois, Convenient and solventless preparation of pure nanotube/polybenzoxazine nanocomposites with low percolation threshold and improved thermal and fire properties, J. Mater. Chem. A 2 (2014) 6814–6822.
[51] L. Dumas, L. Bonnaud, M. Olivier, M. Poorteman, P. Dubois, High performance benzoxazine/CNT nanohybrid network–an easy and scalable way to combine attractive properties, Eur. Polym. J. 58 (2014) 218–225.
[52] L. Dumas, L. Bonnaud, M. Olivier, M. Poorteman, P. Dubois, Facile preparation of a novel high performance benzoxazine–CNT based nano-hybrid network exhibiting outstanding thermo-mechanical properties, Chem. Commun. 49 (2013) 9543–9545.
[53] M. Chapartegui, J. Barcena, X. Irastorza, C. Elizetea, M. Fernandz, A. Santamaria, Analysis of the conditions to manufacture a MWCNT buckypaper/benzoxazine nanocomposite, Compos. Sci. Technol. 72 (2012) 489–497.